International Journal of Geo-Information

MDPI

Article

A Spatial and Temporal Assessment of Vegetation Greening and Precipitation Changes for Monitoring Vegetation Dynamics in Climate Zones over Africa

Vincent Nzabarinda [1,2,3], Anming Bao [1,2,3,4,*], Wenqiang Xu [1,2,3,4], Solange Uwamahoro [1,2,3], Madeleine Udahogora [1,3], Edovia Dufatanye Umwali [1,2,3], Anathalie Nyirarwasa [1,3] and Jeanine Umuhoza [1,2,3]

1 State Key Laboratory of Desert and Oasis Ecology, Xinjiang Institute of Ecology and Geography, Chinese Academy of Sciences, Urumqi 830011, China; vincentnzabarinda@mails.ucas.ac.cn (V.N.); xuwq@ms.xjbt.ac.cn (W.X.); uwamahoroso@mails.ucas.ac.cn (S.U.); udahogorm@mail.ucas.ac.cn (M.U.); umwariedovia@mails.ucas.ac.cn (E.D.U.); rwasan123@mails.ucas.ac.cn (A.N.); umuhoza004@mails.ucas.ac.cn (J.U.)
2 Key Laboratory of GIS & RS Application Xinjiang Uygur Autonomous Region, Urumqi 830011, China
3 University of Chinese Academy of Sciences, Beijing 100049, China
4 Research Center for Ecology and Environment of Central Asia, Chinese Academy of Sciences, Urumqi 830011, China
* Correspondence: baoam@ms.xjb.ac.cn; Tel./Fax: +86-991-788-5378

Abstract: Vegetation is vital, and its greening depends on access to water. Thus, precipitation has a considerable influence on the health and condition of vegetation and its amount and timing depend on the climatic zone. Therefore, it is extremely important to monitor the state of vegetation according to the movements of precipitation in climatic zones. Although a lot of research has been conducted, most of it has not paid much attention to climatic zones in the study of plant health and precipitation. Thus, this paper aims to study the plant health in five African climatic zones. The linear regression model, the persistence index (PI), and the Pearson correlation coefficients were applied for the third generation Normalized Difference Vegetation Index (NDVI3g), with Climate Hazard Group infrared precipitation and Climate Change Initiative Land Cover for 34 years (1982 to 2015). This involves identifying plants in danger of extinction or in dramatic decline and the relationship between vegetation and rainfall by climate zone. The forest type classified as tree cover, broadleaved, deciduous, closed to open (>15%) has been degraded to 74% of its initial total area. The results also revealed that, during the study period, the vegetation of the tropical, polar, and warm temperate zones showed a higher rate of strong improvement. Although arid and boreal zones show a low rate of strong improvement, they are those that experience a low percentage of strong degradation. The continental vegetation is drastically decreasing, especially forests, and in areas with low vegetation, compared to more vegetated areas, there is more emphasis on the conservation of existing plants. The variability in precipitation is excessively hard to tolerate for more types of vegetation.

Keywords: vegetation change; climate zone; rainfall variability; Africa; NDVI3g; persistence index; endangered plants types; Climate Change Initiative Land Cover

Citation: Nzabarinda, V.; Bao, A.; Xu, W.; Uwamahoro, S.; Udahogora, M.; Umwali, E.D.; Nyirarwasa, A.; Umuhoza, J. A Spatial and Temporal Assessment of Vegetation Greening and Precipitation Changes for Monitoring Vegetation Dynamics in Climate Zones over Africa. *ISPRS Int. J. Geo-Inf.* **2021**, *10*, 129. https://doi.org/10.3390/ijgi10030129

Academic Editor: Wolfgang Kainz

Received: 15 December 2020
Accepted: 24 February 2021
Published: 3 March 2021

1. Introduction

Many countries, especially developing countries, depend mainly on agriculture. However, agriculture is also highly dependent on rainfall due to its particular importance for the distribution of certain components of vegetation [1–3]. Despite that, rainfall variability is increasingly becoming a problematic issue that affects food production thus, global hunger is increasing, especially in the aforementioned countries. Nevertheless, the variability of vegetation differs from one climatic zone to another, and its density and health are mainly associated with climate change, human-induced and/or naturally caused. Therefore, similar climatic zones have similar vegetation characteristics, and this classification remains

the key driver of vegetation distribution [4]. Furthermore, in some places, the variability of vegetation and its greening is not related to precipitation variability at all. Therefore, it is extremely important to use climate zones for the spatial-temporal monitoring of vegetation changes. In this way, the calculation of the variation of the vegetation greenness remains a vital element to discover the ecosystem dynamics.

The most widely used method for detecting vegetation greenness is the Normalized Difference Vegetation Index (NDVI) [5,6]. Linear regression models are widely applied to discover the relationship between variables [7], and image regression is one of the many methods used and performed in vegetation studies [8,9]. Linear regression was used to simulate the NDVI trend for each pixel during the study period. Stow, Daeschner [10] used this method to calculate the vegetation's greenness rate of change (GRC). The GRC is defined as the slope of the smallest power-function linear regression equation for the interval changes in the seasonally integrated NDVI during a period. The per-pixel strength of linear association between NDVI and precipitation was determined by calculating the Pearson product moment correlation coefficient (r) for the 34-year time series of yearly observations (1982–2015). The correlation coefficients were calculated between NDVI and precipitation at each pixel during the study period to determine the strength of the relationship between NDVI and this climatic factor. These correlations represented the sensitivity of the regional vegetation to this climatic factor [11–14]. Temporal correlations between NDVI and precipitation were computed to examine the spatial variability of the relationships between those parameters. This helps not necessarily to know what the trigger for individual variation was, but to test how vegetation and precipitation varied over the years.

Considerable studies have been carried out on NDVI–precipitation relationships in Africa, at continental [15–17] and regional scales, for example in the Sahel [18–20], in eastern Africa [21], in central Africa [22], in west Africa [23] and in southern Africa [24,25]. However, these studies have generally focused on average seasonal trends or have only used time series at short intervals. Furthermore, none has assessed its distribution across the continent through climate zones. Additionally, only a few have adopted a comparative approach. To address these gaps, this study used a linear trend model with the purpose of providing a greater understanding on the long-term trajectory (on each pixel) of vegetation change, precipitation variability, and their relationship in Africa through climate zones. The main hypothesis is that African vegetation depends strongly on precipitation, which varies according to climate zone. The specific objectives of this paper are to (1) evaluate the spatial and temporal vegetation and the precipitation trends in different climate zones of Africa, (2) assess the change of greenness in relation to precipitation variability in each climate zone of Africa, and (3) identify the most vulnerable climate zone and vegetation in danger of extinction in different African climate zones. The results generated in this study would therefore show the spatial variations and the distribution pattern of vegetation cover in the different climate zones of Africa. Furthermore, these results will serve as a reference for future assessments of the vegetation-precipitation relationship in the world. Moreover, it will provide a deeper understanding of vegetation response to current precipitation variability and promote the protection of the ecosystem environment. In addition, it will help us to improve predictions of the future consequences of these rainfall variations on ecosystems and enhance the sustainability of greening to strengthen efforts under the impact of rainfall variability in Africa. The remainder of the paper is as follows: the materials and methods in Section 2; the obtained results in Section 3; a discussion in Section 4, and the conclusion in Section 5.

2. Materials and Methods

2.1. Study Area

This study was conducted on the African continent, which represents 6% of the total world's surface area and 20% of the total world's land area. Covering an area of 30.3 million km^2, it is the second largest in the world in terms of area and population after

the Asian continent [26–28]. Geographically, Africa ranges from 17.53282° W, 34.822° S to 57.795409° E, 37.340409° N. This makes it the only continent located in the four hemispheres of the world where the equator and the principal meridian cross. This covers about 54 countries. Africa's climate is very diverse and results from different climate systems [29], and these are arranged into five climate zones, namely, tropical, arid, temperate, cold, and polar climate zones, according to the climate classification by Köppen–Geiger [4]. In Africa, as a warm and dry continent, rainfall patterns largely determine vegetation patterns due to the dependency of plants on water availability [30]. According to the land cover (LC) classification from the European space agency, presented using the LC classification system developed by FAO [31,32], there are 23 types of vegetation in Africa. Among these, nine types are forests, six are vegetation in agriculture areas, three types of sparse vegetation, two types of grasslands, two types of shrubland and one is vegetation in wetlands.

2.2. Datasets

In the continuous monitoring and evaluation of plants evolving on a tremendous spatial and temporal scale, satellite-based remote sensing has continued to prove its effectiveness [29,33]. Among the remote sensing datasets products, NDVI is superior in the use of land degradation and plant health monitoring studies [34,35]. The exceptional time record for terrestrial vegetation dynamics made Normalized Difference Vegetation Index-3rd generation (NDVI3g) the most popular [29]. These NDVI3g datasets were created with an overall NDVI unit level accuracy of 0.005 to solve the problem of calibration loss, orbit drift, and volcanic eruption. These NDVI3g datasets focus on improving calibration and cloud masking [36]. Significantly, they have outperformed many other long-term NDVI datasets [37]. In this regard, the NDVI3g derived from Global Inventory Modeling and Mapping Studies (GIMMS) at a 1/12° resolution integrating data from the National Oceanic and Atmospheric Administration (NOAA) Satellites [38] was chosen for use in this study.

Water and vegetation are closely linked because plants cannot grow or be healthy without water; this is why precipitation is important in our study. The CHIRPS dataset was derived from the climate Hazard Group at University of California, with a 0.5 deg resolution, and was made to answer the problem of geographical coverage [39]. This dataset combines a 0.05 Climate Hazards group precipitation climatology (CHPClim), TIR-based satellite precipitation estimates, and in situ rain gauge measurements [40,41]. During the validation test of the CHIRPS data carried out in West Africa, the CHIRPS products obtained much better performances than those of Africa Rainfall Climatology version2 (ARC2), with a higher skill, low or zero bias, and fewer random errors. They also performed better than the tropical applications of meteorology using satellite data (TAMSAT3) in terms of skill and random error [42]. Based on this, this dataset was chosen for this study. The 24-year coverage and 300-m-spatial-resolution Climate Change Initiative Land Cover (CCLC) dataset derived from the European Space Agency [31,43] made it possible to identify threatened plant species and to determine the fluctuation and succession of all plants as well as their species in Africa per climate zone.

The other data used in this study are Digital Terrain Elevation Data (DTED) from the Shuttle Radar Topography Mission (SRTM) [44]. With the intention of determining the elevation in each climate zone and the altitude in which plants species tend to live, we used the SRTM 90 m, downloaded from http://srtm.csi.cgiar.org/srtmdata/ (accessed on 14 December 2020), with which the mountain and plain were easily identified.

Lastly, to identify the climate zone of Africa, the new global 37-year (1980–2016) maps with a 1 km resolution based on the Köppen–Geiger climate classification [4], were used. These maps are derived from temperature and precipitation and have five climate zones (Figure 1).

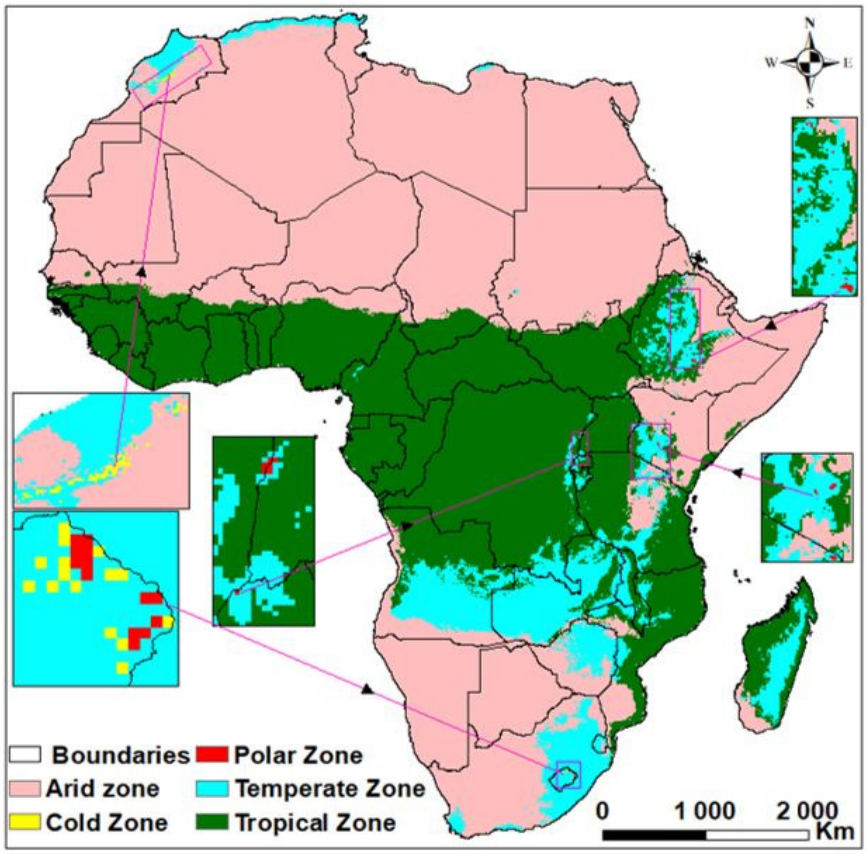

Figure 1. Five climate zones of Africa. This figure is a new figure reusing only some data from [4].

2.3. Methodology

2.3.1. Pre-Processing

The NDVI3g preprocessing involved radiometric correction, geometric correction, cloud extraction and bad-line removal when producing its half-month dataset [45]. The precipitation, LC, and Köppen–Geiger climate classification dataset were all resampled to match the GIMMS data using a bilinear resampling algorithm to preserve the 1/12° spatial resolution of the NDVI3g data [46].

2.3.2. Data Processing

In this study, 816 images of the 16-day NDVI3g GIMMS, 1/12°, for 34 years from 1982 to 2015 in Africa were used. The maximum value composite (MVC) is important for noise removal [47]. Therefore, this method was used to transform the bi-monthly timescale into monthly and annual NDVI3g. Further, a simple linear regression method was used to retrieve long-term trends in inter-annual variations in vegetation. The years were considered independent, and the NDVI3g was used as the dependent variable.

The response of NDVI3g to precipitation variability in each of the five climate zones was expressed as a linearly regressed slope of NDVI3g to the precipitation for each pixel. Statistically, significant testing at the 0.05 levels for linear regression was performed by the F-test.

The Persistence index (PI) of NDVI3g is important for categorizing the consistency of NDVI3g trends [48,49]. Thus, this PI was used to illustrate the evolution of NDVI3g in each of the five climate zones.

$$PI = \sum_{i=1}^{n} PI(i) = PI(1) + PI(2) + \ldots + PI(n) \quad (1)$$

Here, *PI* is the persistence index, (*i*) the time being from 1 to *n*. The linear trends of the average seasonal NDVI3g are calculated for the periods 1982–1984, 1982–1985, 1982–1986, . . . , 1982–2015 and denoted as *t*(*i*), where I = 1, 2, 3, 4, . . . , 32. A score of 1 was assigned at *PI*(*I* + 1) if *t*(*I* + 1) was greater than 80% of *t*(*i*); otherwise, the score was zero. The sum of these scores was then calculated as a PI. The higher the PI, the longer the period of increase in NDVI3g [49].

3. Results

3.1. Evaluation of Statistical Analysis of NDVI3g from 1982 to 2015

The vegetation of Africa is based on the climate zone where the climate has a different influence in each zone, resulting from differences in vegetation type and state. Thus, to better assess the evolution of vegetation through NDVI3g on this continent, it is important to base ourselves on climate zones. Figure 2 below shows the statistical evaluation of the annual averaged NDVI3g in Africa, in each of the five climate zones.

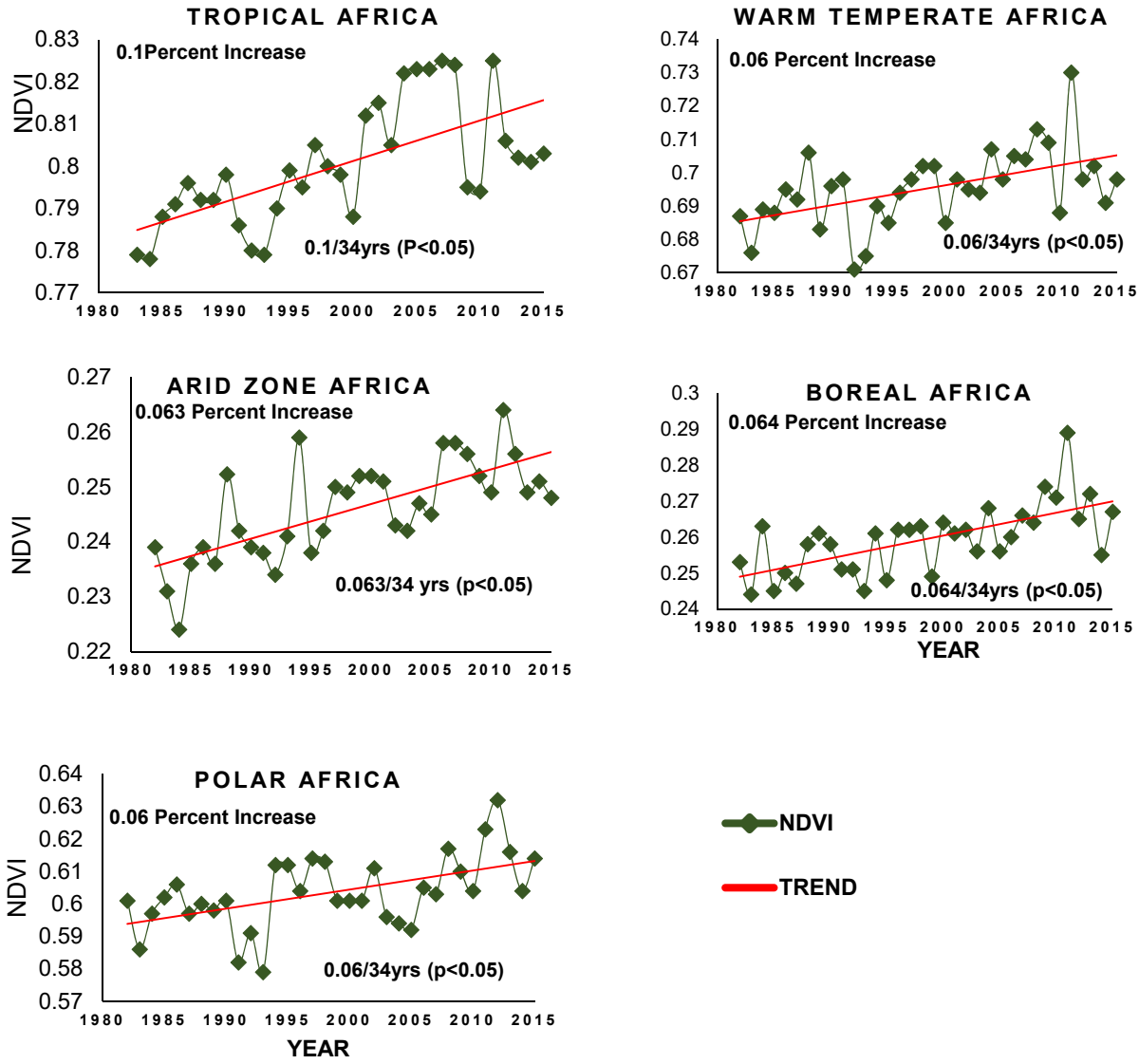

Figure 2. Statistical analysis of Normalized Difference Vegetation Index-3rd generation trends values in all the climate zones of Africa.

In general, based on the NDVI3g statistical figure above, the increase in vegetation greening, in the form of NDVI3g values in all climate zones of Africa, can be provided. The

increase manifested itself in different ways with an exceptionally high change in all climate zones where their annual average NDVI3g values increased from 0.777 (tropical zone), 0.687 (warm temperate zone), 0.239 (arid zone), 0.253 (boreal or cold zone), and 0.601 (polar zone) in 1980 to 0.83, 0.698, 0.248, 0.267, and 0.614, respectively, in 2015. Although there has been uneven vegetation change in each climatic zone, there were astonishing developments in 2011, when the annual average NDVI3g in all climatic zones peaked compared to other years.

In Table 1 below, the NDVI and rainfall columns in each of the five climate zones, the top five NDVI values, and the rainfall values considered special (highest values) were named from 1 to 5 with a fir green color, and the worst five (smallest NDVI and precipitation values) also considered special (worst values), in different years were named from 1 (worst) to 5 with a red color. For each year in every climate zone, we matched NDVI3g with rainfall to clarify the correlation between them. The correlation column with the same climate zones shows the relationship between NDVI and rainfall for each year in every climate zone. For example, the highest NDVI value was found in 2007 and 2011, so a value of 1 in fir green was assigned to these two years; the worst NDVI was discovered in 1982 and thus assigned as 1 in red. These were performed for each climate zone. In the same example, the highest amount of rainfall occurred in 1989, so the year was assigned a 1 in fir green, and 1994 was the lowest in rainfall, so it was assigned a 1 in red color. Of course, due to the small number of years (special from 1 to 5) selected in the long period (1982–2015), some years remained unsigned. Furthermore, the NDVI and rainfall columns overlapped. Green overlaps signify a correlation. Red overlaps indicate a negative correlation (red color). Unsigned values overlapped with assigned values suggest no correlation (black), and the regions where two unsigned values overlap, indicate a corresponding probability. For example, 1983 was red (last five) in terms of NDVI and precipitation (except boreal climate zone for precipitation). Thus, the overlap shows good correlation in the four climate zones. The year 2011 showed a fir green color for all climate zones in terms of NDVI, but there is no sign of precipitation, so there is no correlation between the two. The year 1982 shows a red color for the NDVI in the tropical climate zone, but shows a fir green color for precipitation, and the reverse occurred in 2005, so 1982 and 2005 resulted in a negative (red) correlation.

The NDVI3g and precipitation have been clarified to be very strong from 2004 to 2013 and very low from 1983 to 1987 (excluding 1986 (unsigned) for NDVI3g and 1987(unsigned) for rainfall), and from 1991 to 1993. However, there is a very strong and very low rainfall observed for the periods 1997–1999 and 2014–2015, respectively, in the region with no special NDVI3g. Therefore, regarding the negative and positive correlations, the result revealed five positive correlations (green) and one negative (red) correlation for the period 1982–1984, six positive correlations for the period 1991–1997, and eight positive correlations and one negative correlation from 2004 to 2013. Thus, there is no correlation (black color) for the periods 1985–1990, 1998–2001, and 2014–2015. The polar climate zone obtained the first evidence of a positive (green) correlation between NDVI3g and rainfall (6 years), 1983, 1992, 1993, 1997, 2012, and 2013. The boreal zone was last, because the positive correlation (green) was only revealed in two years (2009 and 2010).

Table 1. The considered special periods during which NDVI3g and rainfall had their highest (five years) and lowest (five years) values and their correlation. Fir green represents high, and red represents low. The numbers 1 to 5 indicate high to low Normalized Difference Vegetation Index (NDVI) and precipitation values (for fir green) and low to high NDVI and precipitation values (for red) in each climate zone. In the correlation column, green represents a positive correlation, black is no correlation, and red is a negative correlation.

	NDVI3g					Rainfall					Correlation				
Years	**T**	**WT**	**P**	**B**	**A**	**T**	**WT**	**P**	**B**	**A**	**T**	**WT**	**P**	**B**	**A**
1982	1					4	1								
1983	4	3	3	1	2	1	3	4		2	1	2	3		4
1984	2				1			1		1					5
1985				3	5										
1986						3			1	3					
1987				4	4										
1988		5						4							
1989		4				1			4						
1990										5					
1991			2												
1992	5	1	4		3	2	4	2		3	1	2	3		4
1993	3	2	1	2				3					5		
1994					2		1		5						
1995				5			2								
1997			5			2	3	1		2			6		
1998									2						
1999						3				5					
2000		5							4						
2001									2						
2004		4		5			5					1			
2005	4		5			5									
2006	5				3		2	5	5	1					2
2007	1				4										
2008	3	2	3		5	5					3				
2009		3		2			4		3			4		5	
2010				4					1	3				6	
2011	1	1	2	1	1										
2012			1					3		4			7		
2013			4	3				2					8		
2014								5							
2015						4	5		3						

Climate zones: T: Tropical, WT: Warm Temperate, P: Polar, B: Boreal and A: Arid.

3.2. Index of Persistence of NDVI3g

The total sum of the calculated PI scores in tropical and arid climate zones of Africa were 28 and 27, respectively, signifying a high PI. The PI in the warm temperate, boreal and polar zones was 24, 23, and 23, respectively, which signifies a low PI.

3.3. Statistical Analysis of the Monthly Mean NDVI3g through the Four Seasons

Table 2 shows the seasonal average for each climate zone in Africa and provides a better understanding of how greenness has developed in each season. It reflects what we discerned in the NDVI3g trend analysis.

Table 2. Statistical Analysis of the mean NDVI3g value throughout four seasons.

	Tropical Zone	Warm Temperate Zone	Polar Zone	Arid Zone	Boreal Zone
(a)	Seasonal mean NDVI3g for four seasons in 1982				
DJF	0.578	0.58	0.507	0.18	0.208
MAM	0.633	0.597	0.499	0.182	0.204
JJA	0.614	0.478	0.458	0.174	0.191
SON	0.632	0.687	0.482	0.181	0.188
(b)	Seasonal mean NDVI3g for four seasons in 2015				
DJF	0.589	0.578	0.495	0.184	0.199
MAM	0.625	0.595	0.462	0.181	0.217
JJA	0.615	0.462	0.448	0.171	0.188
SON	0.659	0.445	0.502	0.182	0.196

3.4. Evaluation of Rainfall Dynamics through Time Series

3.4.1. Rainfall Analysis

The analysis of the precipitation distribution illustrated in Figure 3 shows that precipitation does not match in all climatic zones. Moreover, the increase and decrease in precipitation do not occur simultaneously for distinct climatic zones. However, in some years, the climate zones have low or high precipitation, especially for the peaks of 1985, 2010, and 1997 for all climate zones, except the boreal zone, whereas a low value was common only in 2015 for all climate zones. This reflects the NDVI3g trend by which precipitation was increasing for all climate zones for the periods 1985–1986, 2010–2011, and 1996–1997. It should also be noted that the precipitation is high in the tropical zone as well as the polar zone, very low in the arid zone, low in the boreal zone, and moderate in the warm temperate zone. This sequence does not coincide with the NDVI3g, where the tropical zone is followed by the warm temperate zone, and the polar climate zone is in third place. In addition, the arid zone is the lowest for precipitation and not far from the boreal zone.

Furthermore, the trends for all climate zones in Figure 3 show small but positive slopes, where the polar zone slope is the highest (2.28) and the tropical zone slope is the lowest (0.6). Although it has the smallest slope, it was the only one with a positive intercept (147.5), which means, unlike all other area, it never runs out of rain. This is reflected in Figure 4, where there is a decrease in precipitation in tropical zone, especially in the rainforest zone and parts of Monsoon, which are characterized by a decrease in rainfall at a rate of −22.46 mm each year. Even though these two parts of tropical zone manifested a decrease in precipitation, they have the highest precipitation in Africa (1475.1 mm/year) after the polar zone. Furthermore, part of the tropical zone had the greatest positive trends, increasing to 19.67 mm/year, especially in the rainforest zone, in South Liberia, South East Madagascar, and along East Uganda to West Ethiopia. The semi-arid zone of the tropical zone is generally exhibiting positive trends. Parts of the arid zone, such as the Arid steppe, hot (BSh), and the semi-arid zone, that is to say the parts bordering tropical zone, the boreal, and the warm temperate zone in the northwest demonstrates an upward trend of precipitation at 13.67 mm/year, while the other parts of deserts demonstrate a near-stable rain pattern. The lowest trend rate in both zones was −19.8 mm/year. The rate of warm temperate precipitation ranged from −19.8 to 17.91 mm/year. The decline is mainly identified by its dry summer without a dry season, its dry winter and hot summer, and its dry winter and warm summer in the low elevation areas of the east-southeastern part of South Africa, in the middle to northeastern part of Angola (this part experienced a high degradation trend per NDVI3g), and in North Madagascar, while the increase was demonstrated in parts of Zambia, Southeast Madagascar, North Morocco, Algeria, and Tunisia. The boreal zone, in top mountains (1701–4033 m above sea level) over a small area

between warm tropical and arid zone in the northwest (Central Morocco) and between warm tropical and polar zones in the southeast (Lesotho in South Africa) demonstrates a 13.67 mm/year increase in the northwest and a −19.8 mm/year decrease in the south. The polar zone, in the top of the high mountains (2417–5871 m) above warm temperate and boreal zones (in the south) decreased at −17.77 mm/year and increased at 13.25 mm/year.

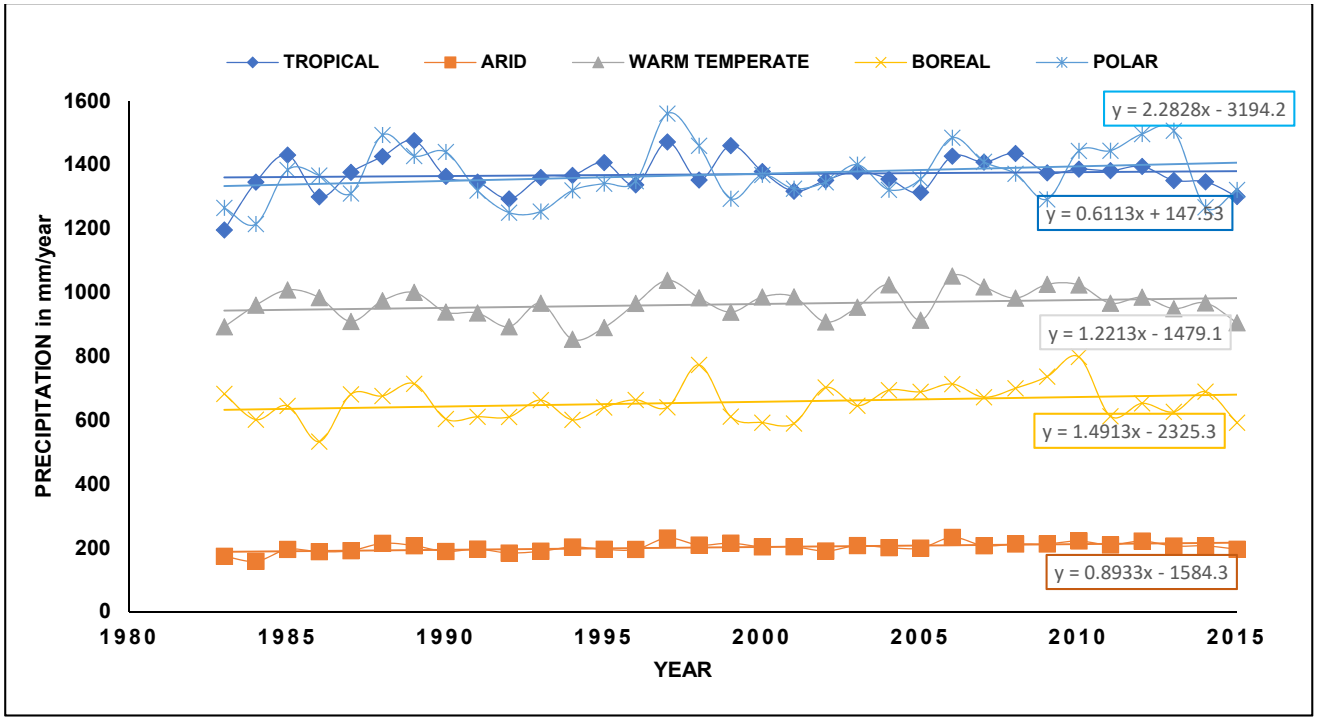

Figure 3. Statistical analysis of mean cumulative rainfall in all the climate zones of Africa from 1982 to 2015.

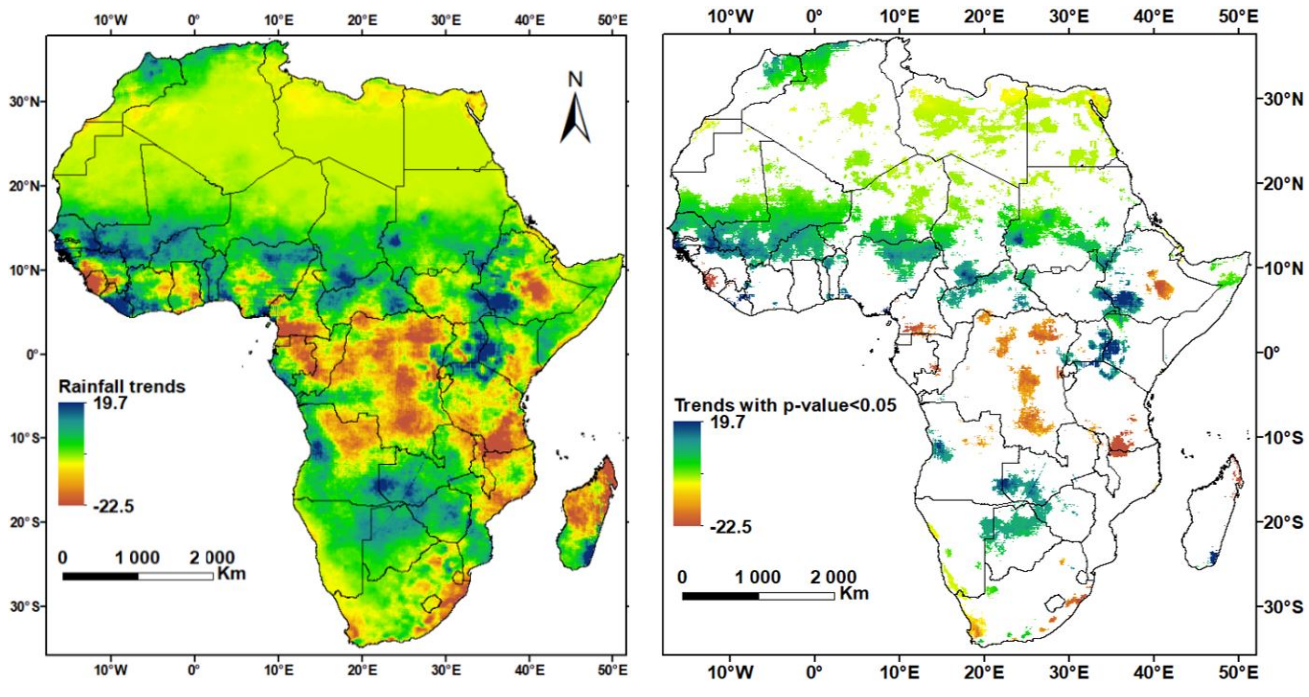

(**a**) (**b**)

Figure 4. African precipitation. (**a**) Spatial distribution of the annual rainfall change trend on each pixel from 1982 to 2015; (**b**) The figure (**a**) with all pixels with non-significant trends (p-value < 0.05) masked out.

Although rainfall appears to have declined in most parts of tropical Africa, such as south Cameroon, northwest Liberia, west Angola, central to East RD Congo and Equatorial Guinea (Figure 4a), most of those areas also experience heavy rainfall (Figure 4b).

Table 3 summarizes the information of our study from 1982 to 2015. The bold numbers are the largest numbers following the rows of elements, while the underlined numbers are the smallest. As the table shows, the polar climate zone is the one located at the highest elevation of 5871 m, and receives high annual precipitation of 1559.7 mm. Contrarily, it is also in an arid climate zone, where the precipitation level is the lowest. An addition to being an arid zone, it is also the one with the lowest mean NDVI3g value. The highest NDVI3g value is found in the tropical climate zone.

Table 3. Summary of altitude, annual mean climate, and NDVI3g data from 1982 to 2015.

	Tropical Zone	**Warm Temperate Zone**	**Polar Zone**	**Arid Zone**	**Boreal Zone**
Elevation (m)(MSL)	−4 to 2675	−3 to 4102	2417 to **5871**	<u>−151</u> to 3330	1701 to 4033
Precipitation (mm)	1195.23 to 1475.1	852.80 to 1051.18	1213.79 to **1559.7**	<u>157.46</u> to 232.4	532.46 to 797.782
NDVI3g	0.78 to **0.83**	0.67 to 0.73	0.58 to 0.63	<u>0.22</u> to 0.26	0.24 to 0.29

Note: The bold numbers are the biggest numbers following the rows of elements while the underline numbers are the smallest.

3.4.2. Precipitation Distribution in Climate Zones from 1982 to 2015

The rainfall in the tropical climate zone increased from 1983 (1195.2 mm) to 1989 (1475.1 mm), which are the lowest and highest precipitation values over the 34 years of the study. After this increase, a sharp decrease was observed from 1989 to 1992, which was followed by a complex increase until 1999. From 1999 to 2005, there was a complex decrease, and there was then increase from 2005 to 2008. The rainfall declined from 2008 to 2015. However, during this last period, rain increased for three years (2009–2012), resulting in a greater amount of vegetation greenness.

In the arid climate zone, rainfall increased from 1984 (157.46 mm) to 1988 (213.58 mm), which are the lowest and highest precipitation values over the 34 years of the study. After this increase, it decreased from 1988 to 1992, followed by a complex increase lasting until 1997, a complex decrease from 1997 to 2002, an increase from 2002 to 2006. Further, rainfall declined from 2006 to 2015. However, during this last period, rains increased for three years (2007–2010). The year 1984 was the weakest in terms of precipitation, resulting in the least greenness of vegetation. In decreasing order, the five best years of precipitation were 2006, 1997, 2010, 2012, 1999, and 1988. The worst five years were 1990, 1986, 1992, 1983, and 1984.

In the warm temperate zone, rainfall increased from 1983 (1195.2 mm) to 1989 (1475.1 mm), which are the lowest and highest precipitation values over 34 years of the study. After this increase, a sharp decrease was observed from 1989 to 1992, which was followed by a complex increase lasting until 1999 and a complex decrease from 1999 to 2005. An increase was observed from 2008 to 2009, rainfall declined from 2006 to 2015. The year 2006 has the highest rainfall, resulting in greater vegetation greenness.

In the boreal climate zone, rainfall decreased from 1983 to its lowest level over the 34 years of the study and increased from 1986 to 1989. After this increase, it decreased from 1989 to 1994 and then increased until 1998. From 1998 to 2001, there was a direct drop and then an increase from 2001 to 2010. Further, rainfall declined from 2010 to 2015. However, vegetation greenness in this climate zone showed its best index in 2011, and 2010 had the highest rainfall.

Precipitation in the polar climate zone increased mainly from 1984 to 1988. After this increase, a direct decrease was observed from 1988 to 1992, followed by a direct

increase to its maximum amount in the 34 years of the study in 1997 (1559.7 mm). The complex precipitation decreased from 1997 to 2015, but was divided into small increases and decreases: a decrease from 1997 to 1999, an increase from 1999 to 2006, a sharp decrease from 2006 to 2009, and an increase from 2009 to 2013. A sharp decrease was observed from 2013 to 2014, where precipitation decreased from 1506.1 to 1266.6 mm.

Generally, all climate zones experienced a common reduction in precipitation from 1989 to 1992. This was followed by an increase lasting until 1997 and then a decrease lasting until 2001. By integrating the complex evolution of precipitation, rainfall can be classified into two phases, increasing and decreasing respectively, from 1983 to 1989 and from 1989 to 2015 in the tropical zone, from 1983 to 2006 and from 2006 to 2015 in the arid zone, from 1983 to 2006 and from 2006 to 2015 in the warm temperate zone, from 1983 to 2010 and from 2010 to 2015 in the boreal climate zone, and from 1983 to 1997 and from 1997 to 2015 in the polar climate zone.

3.5. Analysis of Vegetation Trend Dynamics

Based on the linear model results, the NDVI3g trends from 1982 to 2015 for each pixel value showed (Figure 5) an annual rate of increase up to 0.013 and a decrease down to −0.014. Astonishingly, the sharp increase up to 0.013 rate per year was found in the arid climate zone. It is in this climate zone where the maximum and minimum rates of vegetation have been discovered (Figure 6). In the semi-arid zone (boundary of the desert hot zone and steppe hot zone) along the Sahel belt, the vegetation shows an increasing growth rate up to 0.013/year. Looking at the overall climate zones in Africa, there was an annual increase in verdant vegetation, where the smallest percentage of increase was found in the temperate zone with 67.6%. We must not overlook the fact that there was a marked decline down to −0.014 each year in arid, desert, hot (BWh) zones in different countries such as Angola, North Botswana, Southeast Sudan, and Somalia (Figure 5).

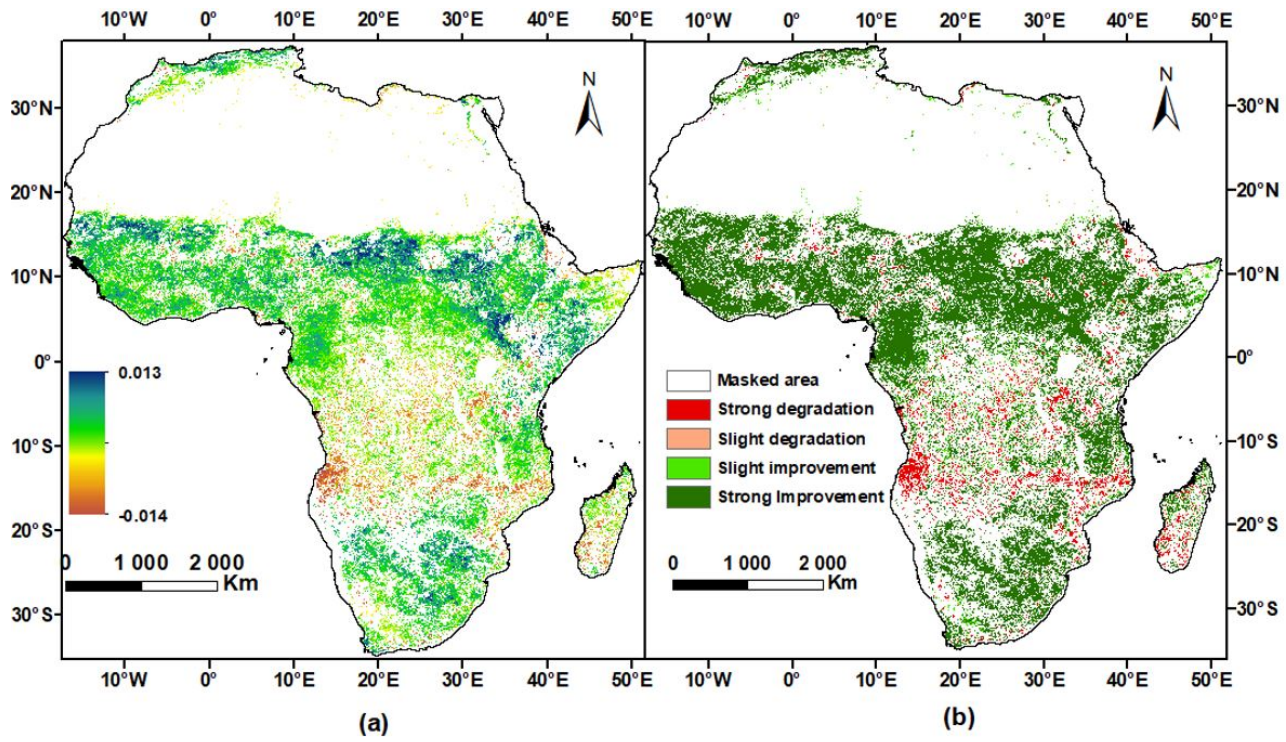

Figure 5. Overall trends of Annual NDVI3g for 34 years of the study (1982 to 2015). (**a**) Shows the overall trends of annual NDVI3g in terms of year; (**b**) shows classified overall trends into four classes: Strong degradation from −0.014 to −0.001/year, slight degradation from −0.001 to 0, slight improvement from 0 to 0.001, strong improvement from 0.001 to 0.013/year. Only significant values (<0.05 of *p*-Value) are mapped. This figure is adapted based on the original figure from publication [50].

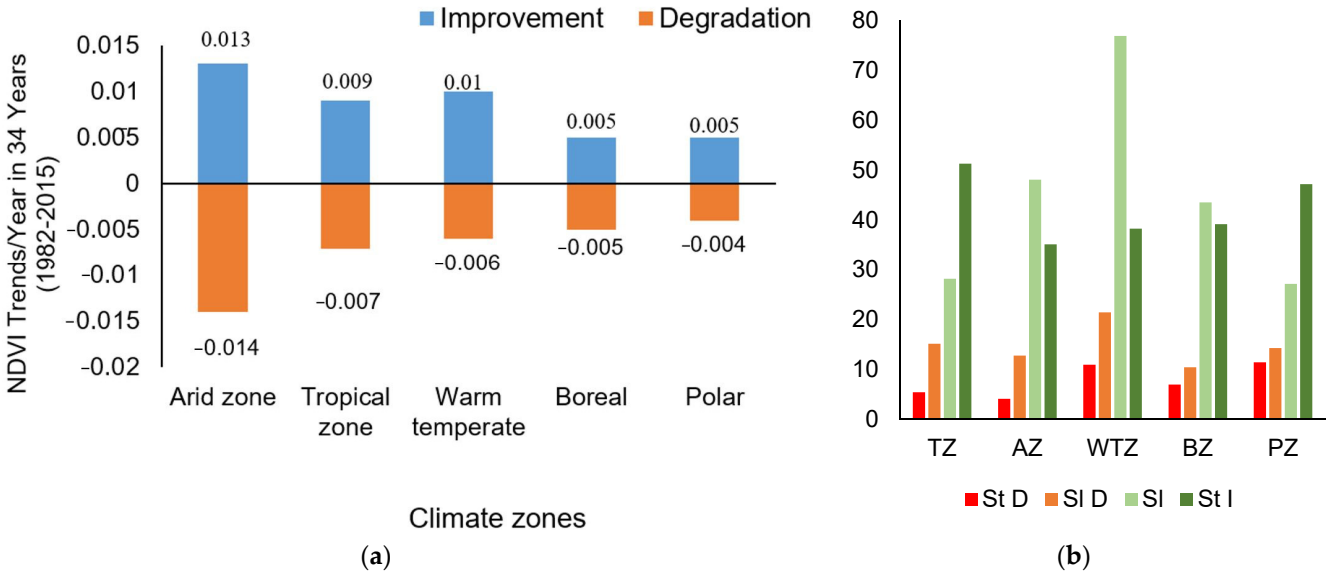

Figure 6. Overall trends in annual NDVI3g in each of the five climate zones of Africa. (**a**) the rate of increase and decrease per year; (**b**) the statistical results' area in percentage of greening variation from 1982 to 2015, with St D: Strong Degradation, Sl D: Slight Degradation, SI: Slight Improvement and St I: Strong Improvement; AZ: Arid Zone, TZ: Tropical Zone, Wt Z: Warm Temperate, PZ: Polar Zone and BZ: Boreal Zone.

Figure 6 summarizes (a) the overall trends in each climate zone of Africa, showing a strong degradation (−0.014, −0.007, −0.006, −0.005, and −0.004) moving to a strong improvement (0.013, 0.009, 0.01, 0.005, and 0.005) in the arid, tropical, temperate, boreal and polar zones, respectively, and (b) the statistical analysis on the status of vegetation condition in each climate zone of Africa, following the vegetation variation. From this, 83.3%, 83.1%, 79.4%, 72.9% and 67.6%, experienced improvement in the boreal, arid, tropical, polar and temperate zones, respectively.

3.6. Change Detection for Each Type of Vegetation per Pixcel Value

Figure 7 shows the areas in % improved and degraded generally in all study area and the annual average rate of change of vegetation for individual vegetation types in each climate zone of Africa. Generally, the vegetation class 60 was decreased to −74% amid strong degradation and −37% amid slight degradation and 60 in the improvement area was mostly reduced, while −3.9% in strong improvement area reduced to 8.4%. Seven types of vegetation degraded in the tropical climate zone, and the four most degraded vegetation classes were 120, 40, 50, and 60 at a rate of −0.86, −0.23, −0.15 and −0.07 values of pixel unity (PU) in 24-year, and the 16 vegetation classes increased, five of which 62, 10, 11, 30 and 100 increased at a rate of 0.39, 0.26, 0.19, 0.14 and 0.1 PU, respectively. In the arid zone, eight types of vegetation were degraded, the highest of which was 190 with −0.22 PU followed by 150, 120, 110, 100, 60, 122, and 50 classes with rates of −0.09, −0.08, −0.06, −0.02, −0.01, −0.003-, and −0.0005 PU, respectively. The highest four among the Seventeen vegetation classes increased by 0.12, 0.1, 0.05, and 0.08 PU are class 10, 11, 153, and 130, respectively. In the warm temperate region, nine were degraded at a rate of up to −0.13. 60 at −0.13 PU, followed by 120 at −0.036 PU. The highest increase among the 14 classes was at a rate of up to 0.08 PU, and the first was class 11, followed by 10 (0.04 PU) and 100 (0.03 PU). In the boreal climate zone, five degraded, of which the two largest were 110 and 190 at −0.004 and −0.0006 PU, and six improved vegetation classes, two of which were 150 and 153 at 0.003 and 0.002 PU. In the polar zone the rate of vegetation change was very small; one degraded vegetation class was 50 at −0.00003 PU, and seven improved, one of which was 62 at 0.00003 PU.

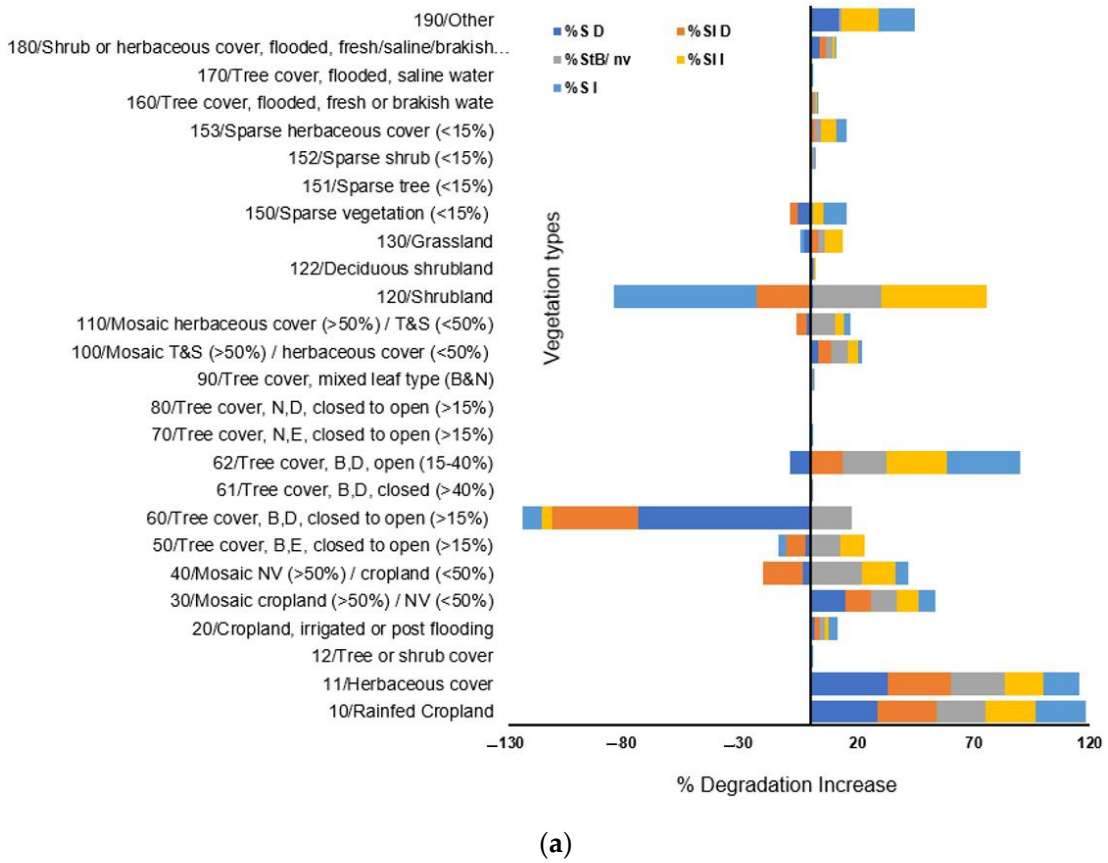

(**a**)

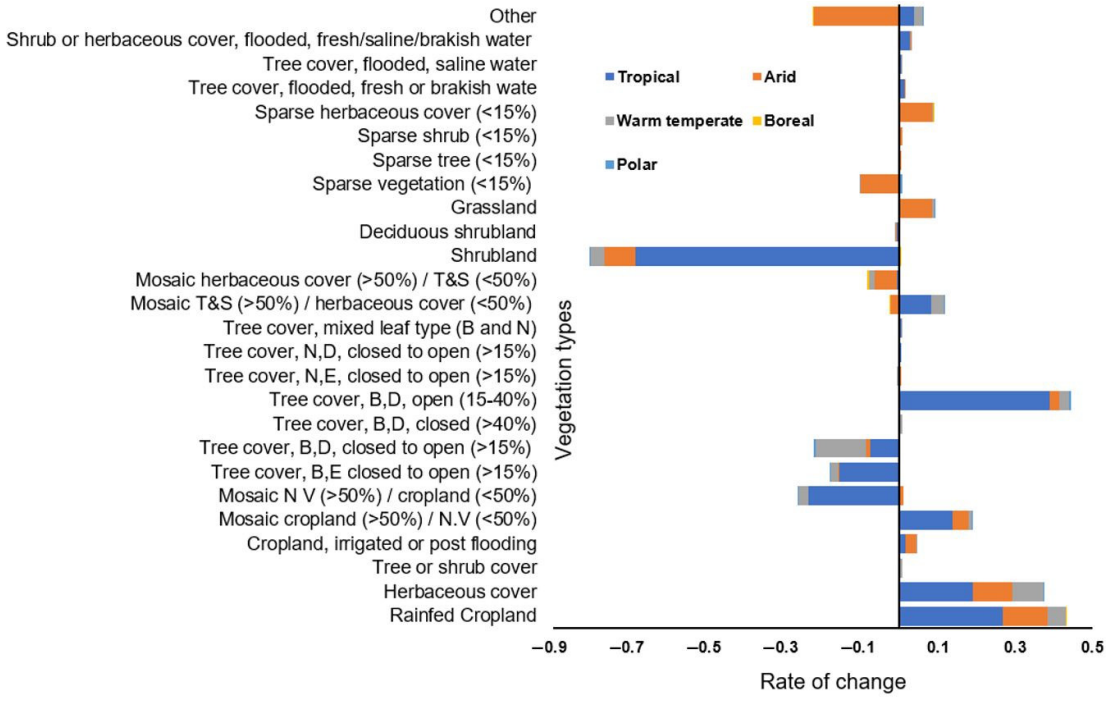

(**b**)

Figure 7. Chart of Vegetation Change (**a**) trends in % and (**b**) rate of change from 1992 to 2015. With, %S D: is % of Strong degradation, %SI D: % of Slight degradation, %StB/nv: % of Stable or non-vegetation, %Sl I: % of Slight Improvement, %S I: % of Strong Improvement. Where, NV: natural vegetation; B, E: broadleaved, evergreen; B, D: broadleaved, deciduous; N, E: needle leaved, evergreen; N, D: needle leaved, deciduous; B & N: broadleaved and needle leaved; T&S: tree and shrub. Other (Urban areas, Bare areas, Consolidated bare areas, Unconsolidated bare areas, Water bodies).

3.7. Consistency between NDVI3g and Precipitation Interannual Variation

Precipitation and vegetation have a special relationship because of the dependence of plants on water availability. When it rains, the grass softens and turns green. However, that does not prevent the no green vegetation to depend on precipitation too, perhaps because of the climate in which they are found. Therefore, each vegetation no matter where it is, depends on precipitation.

The correlation coefficient between NDVI3g and precipitation demonstrated differently in the five climate zones of Africa (Figures 8 and 9). About 69.5% of the total NDVI3g covered was positively correlated with precipitation. The tropical rainforest correlated from −0.55 to 0.57; 51.26% correlated positively, 39.68% were slightly correlated. The tropical monsoon was from −0.63 to 0.78, with only a 47.49% positive correlation and 38.7% were slightly correlated. The tropical savannah correlates from −0.67 to 0.80, and 62.44% of the vegetation cover is positively correlated with precipitation, with 51.12% slightly correlated. In general, the tropical zone revealed a positive correlation of 59.87%, and only 1.02% were strongly correlated, which was discovered mainly in Savannah. The arid climate zone shows a 76.91% positive correlation, 53.7% of which was a slight correlation. From this, the Arid desert hot (BWh) correlated from −0.774 to 0.93 has a 67.55% positive correlation, 45.83% of which is slightly correlated and 15.85% of which is strongly correlated. Most of this correlated part is on the limit of the semi-arid zone of the Sahel belt, the horn of Africa, and the west-southwest part (Figure 9). Correlated from −0.43 to 0.88, the arid desert cold (BWk) shows a 95.76% positive correlation, 72.15% of which was slightly correlated and 21.5% of which correlated strongly. The NDVI3g in the Arid steppe hot (BSh) which is mainly in the semi-arid zone, positively correlated with rainfall from −0.6 to 0.85 at 94.37%, 67.96% of which is a slight correlation and 23.52% of which is a strong correlation. Finally, the Arid steppe cold (BSk) varied from −0.53 to 0.81, and showed a positive correlation at 95.33%, 70.15% of which were slightly correlated and 23.13% of which were strongly correlated. The warm temperate climate zone correlated from −0.62 to 0.75, and 65.15% was positively correlated between the NDVI3g and the precipitation, of which 53.3% was slightly correlated and 3% of which was strongly correlated. Among the nine sub-zones of this climate, the temperate, no dry season, hot summer (Cfa) was 50% positively correlated and 44.4% negatively correlated. Further, the correlation of the last two mountain climate zones was more positive than negative. In the boreal climate zone, 83.48% is positively correlated, of which 2.6% and 66.96% showed strong and slight positive correlations, respectively. In the polar climate zone, 61.43% was positively correlated, while 38.57% showed a negative correlation between NDVI3g and precipitation.

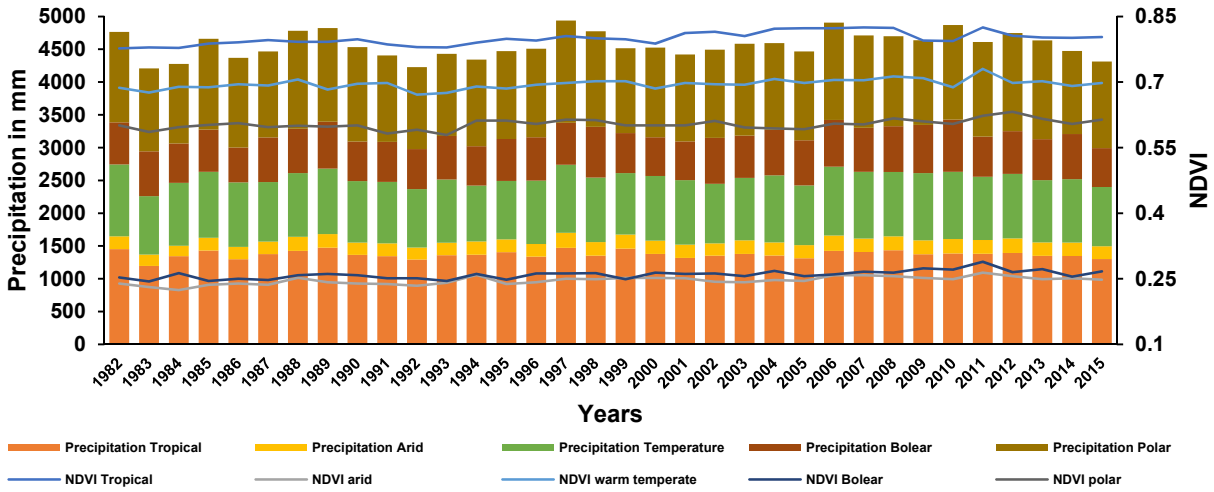

Figure 8. Consistency Between NDVI3g and Precipitation interannual variation in all African climate zones in 34 years of the study.

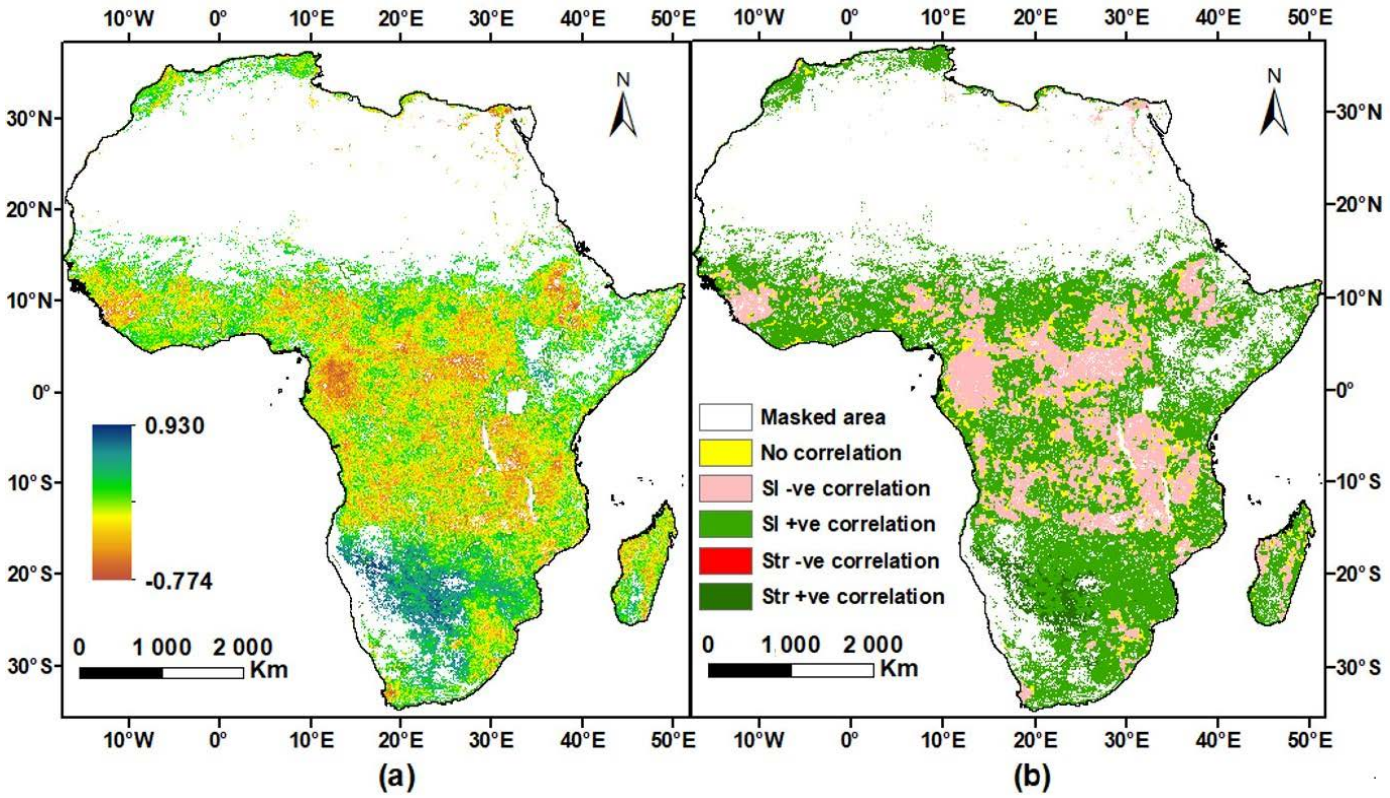

Figure 9. The only significance (from −0.05 to 0.05 p-value) Spatial distribution of the correlation coefficient between inter-annual NDVI3g and Rainfall from 1982 to 2015. (**a**), original correlation coefficient; (**b**), classified into five classes as from −0.774 to −0.5: strong(str) negative(-ve) correlation, −0.5 to −0.05: slight (Sl) negative (-ve) correlation, −0.05 to 0.05: no correlation, 0.05 to 0.5 slight (Sl) positive (+ve) correlation, 0.5 to 0.930: strong (Str) positive (+ve) correlation.

4. Discussion

4.1. Vegetation Trend Analysis from 1982 to 2015

An upward trend of vegetation from 1982 to 2015 was revealed, and a reasonably clear greening trend is evident throughout the Sahel belt, which is consistent with previous studies [29,50–53]. During this period, rainfall in this region increased significantly (Figure 4), indicating that the greening trend can be interpreted as a drought recovery that hit the region in the early 1980s [29,54,55]. This increase could also result from the Great Green Wall (GGW) reforestation project in the Sahel belt in 2005 [56] in response to desertification, soil degradation, food security and climate change [57].

Depending on the study period, the highlighted period is from 2005 to 2013, more especially in 2011, which was the year in which vegetation experienced the greatest greenness in almost all climate zones (Figure 8). However, 2005 was among the five worst, and 2007 was not good for polar climate vegetation. For the periods 1996–1998 and 2001–2002, the vegetation of all climate zones also experienced good greening trends. Among these periods, the best in the tropical climate zone were observed in 2007 and 2011, it was 2012 in the polar zone, and it was 2011 in the warm temperate, boreal, and arid climate zones. On the contrary, vegetation was worst during the periods from 1982 to 1984 and from 1991 to 1993. The greenness of the African vegetation almost entirely degraded at a high level (Table 1). This is associated with the drought that occurred in most African countries from 1981 to 1985 [58] and from 1991 to 1993 [59]. The greatest increase in vegetation in the tropical climate zone occurred in 2007 and 2011 and the lowest value of vegetation greenness was in 1982. There is no evidence resulting from heavy or light rainfall because observed rainfall in 2007 and 2011 was normal, showing only an increase over the previous year. The evidence that precipitation was low is linked to the drought that occurred from July 2011 to August 2012 in East Africa [60,61]. Although 1982 was identified as the year

with the lowest vegetation greening, it was marked by heavy precipitation (Figure 3 and Table 1), and the lowest value was unrelated to precipitation, as it was high in 1982 and increased from 1983 to 1985. This may have the effects of one of the three longest and most powerful El Niño condition in 1982/1983 [62].

Generally, the vegetation of the tropical zone increased from 1982 to 2015, but degraded significantly during the periods 1982–1984 and 1992–1993 while strongly increased from 2005 to 2008 and in 2011. The increase and decrease in vegetation were mainly related to rainfall; for example, the decrease from 1991 to 1993 resulted from a decrease in rainfall from 1988 to 1992. The exception is in 1982 and 2005; rainfall was high in 1982 but NDVI was low, and NDVI was high in 2005 but rainfall was low.

In 1983 and 1992, for all climate zones except the boreal, vegetation degraded due to the low precipitation (Table 1, Figures 3 and 8). In 1993, with the exception of the arid zone, all climate zones suffered from vegetation degradation, but only the polar climate zone experienced a very low precipitation. In 1997, in all climate zones except the boreal zone, we observed heavy precipitation, but only the polar zone showed good vegetation. In 2005, the tropical climate zone was among the top five highest values in terms of vegetation, while it was among the worst five in terms of precipitation. In 2006, all climate zones except the tropical zone had heavy rainfall. However, the arid and tropical zones had good vegetation. The precipitation in the tropical zone was high, but not in the top five. In 2011, all climate zones had good vegetation, but there was no evidence of good precipitation (Table 1). Our results are in line with that of Davis-Reddy [29], who identified positive NDVI anomalies in 1997, 2006, and 2011 due to good precipitation.

The results in 1 also show that, except the polar climate zone in which vegetation degradation was observed in 2005, all climate zones experienced good vegetation from 2004 to 2013. This is consistent with Davis-Reddy [29], who reported that the 2000s were wetter in almost all of Africa. In 1988, the warm temperate zone had good vegetation; however, in the following year, it was highly degraded. This vegetation had not shown any relationship with rainfall. The worst vegetation degradation was observed in 1984 in the tropical and arid climate zones, and this year had the lowest rainfall in the arid and polar regions, but this did not occur in the last five periods of low rainfall in the tropical climate zone. However, 1983 had the lowest rainfall, and 1984 was also within the eight years of the lowest precipitation in this climate zone. The worst vegetation and the lack of precipitation observed here resulted from the strong drought conditions from 1983 to1985 [29,63]. The lowest rainfall in the polar zone was observed in 1984, but this year shows normal vegetation. The strongest degradation was observed in 1993 and was associated with the very low rainfall that lasted from 1992 to 1993. It is obvious that this was resulted from the 1991/1992 drought in South Africa [29].

Each climate zone has shown a sequence of at least two years for the best and worst vegetation events, which sometimes coincided with rainfall events (Figure 8). The best occurred from 2005 to 2008 and in 2011 in the tropical zone, from 2008 to 2009 and in 2011 in the temperate zone, from 2011 to 2013 and in 2008 in the polar zone, from 2009 to 2011 and in 2013 in the boreal zone, and from 2006 to 2008 and in 2011 in the arid climate zone. This resulted from the positive rainfall anomalies observed over the large part of sub Saharan Africa in the 2000s [29].

Figure 7 shows the vegetation types in the four aggregate trend groups of NDVI3g. Four forest types (50, 60, 62 and 170), two grassland types (110 and 130), one sparse vegetation type (150), and vegetation type (40) were severely degraded. Regarding slight degradations, except for 62 among the forest types mentioned above, a grassland type (110), sparse vegetation (150), and vegetation type (40) were all degraded, including shrubland (120 and 122) and bare areas. There was no decrease in stable or non-vegetated area, which proves the accuracy of our results. Regarding slight improvements, fluctuations in vegetation were observed where only 3 (60, 61, and 152) types of vegetation were degraded at 4%, 0.1%, and 0.2% respectively. Further, vegetation also showed strong improvement,

where six types of vegetation (50, 60, 61, 120, 122, and 130) were degraded by 3.2%, 8.4%, 0.14%, 61.3%, 0.78%, and 1.4%, respectively.

The NDVI, however, reveals restrictions in detecting and attributing changes in vegetation cover due to factors that can negatively bias NDVI-based estimates of plant biomass, such as dust deposition [64] and soil background [65] in the arid zone. These areas were masked.

4.2. Analysis of Vegetation by Index of Persistence

The level of persistence refers to the level at which the ecosystems studied are governed by positive feedback mechanisms tending to destabilize the system by external forces. In this feedback framework, the concept of persistence is extremely applicable for characterizing the stability/instability properties of the vegetation dynamics [66–68]. In our case, the dynamics of tropical vegetation were found to be the most stable, followed by the arid climatic zone. This stability indicates a successive longer period of increasing vegetation. The other three climate zones showed low stability through the PI. This explains the high vegetation variability in these climatic zones, which may have resulted from the high rain fall variability.

4.3. Correlation Coefficient between NDVI3g and Precipitation from 1982 to 2015

According to the results, looking at the positive and negative correlation rates, it is clear that there is a good relationship between African vegetation and precipitation when the overall positive correlation was about 80% of the study area (Figure 9).

The results revealed that vegetation is mainly affected by rainfall in the semi-arid regions of Africa, which include Morocco, Northern Algeria, the Sahel belt, Southern Africa, and East Africa (Figure 9). These regions are marked by low annual precipitation and the primary restriction to plant development is the water availability [69]. Our results are consistent to those reported by other studies previously [29,70–72]. Furthermore, this strong correlation implies that the vegetation productivity in these regions is highly dependent on precipitation [69,70].

All climate zones showed more positive correlations than negative correlations between vegetation and rainfall. The Boreal zone was the most correlated zone at 83.48%, followed by the arid zone at 65.15%, the temperate zone at 65.155 %, the polar zone at 61.43%, and the tropical zone at 59.87%. The cold, arid, and temperate zones have annual rainfall below 1000 mm. This is consistent with the result of Davenport and Nicholson [73], who concluded that, when annual rainfall is below around 1000 mm, there is a strong correlation between temporal and spatial NDVI trends. Although the vegetation of the tropical zone is the most greening, many parts of the zone did not show a positive correlation, which are the same areas that showed a high negative trend (Figure 4) in precipitation throughout the study period.

5. Conclusions

Based on this study following these climate zones, the dynamics of vegetation greenness in Africa has evolved over the past 34 years (1982–2015). With the help of NDVI3g, using a linear regression model, the greening trend of the vegetation in terms of years was evaluated, and the results show that it increased at a rate of 0.013/year. This does not exclude areas where decline occurred at a rate of 0.014/year. Some of these vegetation changes were short-term. We measured the PI for each climate zone. Short-term vegetation changes were observed in the warm temperate, boreal, and polar climate zones, as shown by a low PI of 24, 23, and 23, respectively. Tropical and arid zones demonstrated a high PI of NDVI (28 and 27), respectively, which means that these two zones experienced a long-term change in NDVI. Thus, these two regions experienced a relatively long period of increase in NDVI3g. We tested the effect of precipitation on the increasing and decreasing of vegetation greenness, by applying Pearson's correlation coefficients between CHIRPS and NDVI3g. The results showed a higher positive correlation (0.93) rate than a negative

(−0.774). The negative rate was found in the areas with negative trends in precipitation but that normally experienced heavy rains, mainly in Central Africa and some parts of West Africa, such as Sierra Leone, Guinea and, Central Nigeria. This also was found in East African countries such as Malawi, the western part of Tanzania, and the northern part of Ethiopia. To identify the types of threatened plants, LC datasets were used, and the results showed that the highly degraded area was mainly associated with Tree cover, broadleaved, deciduous, closed to open (>15%) forest type, strongly degraded at 74% of its initial total area. In areas of strong improvement, it was observed that shrubland was mainly devastated (61% of its initial total area removed) and in the favor of agriculture activities (Rainfed Cropland, herbaceous cover, etc.). It is clear that the continental vegetation is dramatically decreasing, especially forests. Further, it has been shown that there is a greater conservation of plants in less-vegetated areas than in areas with more vegetation. It has been also clarified that precipitation is highly variable, and few plants can tolerate these fluctuations.

Author Contributions: Design, Investigation and Supervision, Vincent Nzabarinda, Anming Bao and Wenqiang Xu; Conceptualization, Solange Uwamahoro, Madeleine Udahogora, Edovia Dufatanye Umwali, Anathalie Nyirarwasa and Jeanine Umuhoza; Software, Methodology and Writing original draft, Vincent Nzabarinda; Solange Uwamahoro. The positive suggestions of the final manuscript have been read and contributed by all the authors. All authors have read and agreed to the published version of the manuscript.

Funding: This research was funded by the National Program on Key Basic Research Project of China, Grant number 2018YFE0106000 and Science and Technology Partnership Program, Ministry of Science and Technology of China, Grant number KY 201702010.

Institutional Review Board Statement: Not applicable.

Informed Consent Statement: Not applicable.

Data Availability Statement: The source of all the data used in this study is provided in the manuscript.

Acknowledgments: The financial support and research lab facilities for this study were from Chinese government, Xinjiang Institute of Ecology and Geography, (UCAS), Urumqi 830011 and University of Chinese Academy of Sciences (UCAS), Beijing. The authors are very grateful to National Aeronautics and Space Administration (NASA), the United States geological survey (USGS) and European Space Agency (ESA) Climate Change Initiative (CCI) Land Cover project for their data. Further, the acknowledgment is directed to reviewers for their comments and suggestions.

Conflicts of Interest: The authors declare no potential conflict of interest to affect this reported work.

References

1. Platts, P.J.; McClean, C.J.; Lovett, J.C.; Marchant, R. Predicting tree distributions in an East African biodiversity hotspot: Model selection, data bias and envelope uncertainty. *Ecol. Model.* **2008**, *218*, 121–134. [CrossRef]
2. Bucini, G.; Hanan, N.P. A continental-scale analysis of tree cover in African savannas. *Glob. Ecol. Biogeogr.* **2007**, *16*, 593–605. [CrossRef]
3. Greve, M.; Lykke, A.M.; Blach-Overgaard, A.; Svenning, J.-C. Environmental and anthropogenic determinants of vegetation distribution across Africa. *Glob. Ecol. Biogeogr.* **2011**, *20*, 661–674. [CrossRef]
4. Beck, H.E.; Zimmermann, N.E.; McVicar, T.R.; Vergopolan, N.; Berg, A.; Wood, E.F. Present and future Köppen-Geiger climate classification maps at 1-km resolution. *Sci. Data* **2018**, *5*, 180214. [CrossRef]
5. Gascon, M.; Cirach, M.; Martínez, D.; Dadvand, P.; Valentín, A.; Plasència, A.; Nieuwenhuijsen, M.J. Normalized difference vegetation index (NDVI) as a marker of surrounding greenness in epidemiological studies: The case of Barcelona city. *Urban For. Urban Green.* **2016**, *19*, 88–94. [CrossRef]
6. Rhew, I.C.; Stoep, A.V.; Kearney, A.; Smith, N.L.; Dunbar, M.D. Validation of the normalized difference vegetation index as a measure of neighborhood greenness. *Ann. Epidemiol.* **2011**, *21*, 946–952. [CrossRef]
7. Uyanık, G.K.; Güler, N. A study on multiple linear regression analysis. *Procedia Soc. Behav. Sci.* **2013**, *106*, 234–240. [CrossRef]
8. Nordberg, M.-L.; Evertson, J. Vegetation index differencing and linear regression for change detection in a Swedish mountain range using Landsat TM® and ETM+® imagery. *Land Degrad. Dev.* **2005**, *16*, 139–149. [CrossRef]

9. Luppino, L.T.; Bianchi, F.M.; Moser, G.; Anfinsen, S.N. Unsupervised image regression for heterogeneous change detection. *IEEE Trans. Geosci. Remote Sens.* **2019**, *57*, 9960–9975. [CrossRef]
10. Stow, D.; Daeschner, S.; Hope, A.; Douglas, D.; Petersen, A.; Myneni, R.; Zhou, L.; Oechel, W. Variability of the seasonally integrated normalized difference vegetation index across the north slope of alaska in the 1990s. *Int. J. Remote Sens.* **2003**, *24*, 1111–1117. [CrossRef]
11. Broge, N.H.; Leblanc, E. Comparing prediction power and stability of broadband and hyperspectral vegetation indices for estimation of green leaf area index and canopy chlorophyll density. *Remote Sens. Environ.* **2001**, *76*, 156–172. [CrossRef]
12. Major, D.J.; Baret, F.; Guyot, G. A ratio vegetation index adjusted for soil brightness. *Int. J. Remote Sens.* **1990**, *11*, 727–740. [CrossRef]
13. Lyon, J.G.; Yuan, D.; Lunetta, R.S.; Elvidge, C.D. A change detection experiment using vegetation indices. *Photogramm. Eng. Remote Sens.* **1998**, *64*, 143–150.
14. Duan, H.; Yan, C.; Tsunekawa, A.; Song, X.; Li, S.; Xie, J. Assessing vegetation dynamics in the Three-North Shelter Forest region of China using AVHRR NDVI data. *Environ. Earth Sci.* **2011**, *64*, 1011–1020. [CrossRef]
15. Scanlon, T.M.; Albertson, J.D.; Caylor, K.K.; Williams, C.A. Determining land surface fractional cover from NDVI and rainfall time series for a savanna ecosystem. *Remote Sens. Environ.* **2002**, *82*, 376–388. [CrossRef]
16. Lotsch, A.; Friedl, M.A.; Anderson, B.T.; Tucker, C.J. Coupled vegetation-precipitation variability observed from satellite and climate records. *Geophys. Res. Lett.* **2003**, *30*. [CrossRef]
17. Zhang, X.; Friedl, M.A.; Schaaf, C.B.; Strahler, A.H.; Liu, Z. Monitoring the response of vegetation phenology to precipitation in Africa by coupling MODIS and TRMM instruments. *J. Geophys. Res. Space Phys.* **2005**, *110*. [CrossRef]
18. Fensholt, R.; Rasmussen, K.; Kaspersen, P.; Huber, S.; Horion, S.; Swinnen, E. Assessing land degradation/recovery in the African Sahel from long-term earth observation based primary productivity and precipitation relationships. *Remote Sens.* **2013**, *5*, 664–686. [CrossRef]
19. Lee, E.; He, Y.; Zhou, M.; Liang, J. Potential feedback of recent vegetation changes on summer rainfall in the Sahel. *Phys. Geogr.* **2015**, *36*, 449–470. [CrossRef]
20. Georganos, S.; Abdi, A.M.; Tenenbaum, D.E.; Kalogirou, S. Examining the NDVI-rainfall relationship in the semi-arid Sahel using geographically weighted regression. *J. Arid Environ.* **2017**, *146*, 64–74. [CrossRef]
21. Kalisa, W.; Igbawua, T.; Henchiri, M.; Ali, S.; Zhang, S.; Bai, Y.; Zhang, J. Assessment of climate impact on vegetation dynamics over East Africa from 1982 to 2015. *Sci. Rep.* **2019**, *9*, 1–20. [CrossRef]
22. Rousvel, S.; Armand, N.; Andre, L.; Tengeleng, S.; Alain, T.S.; Armel, K. Comparison between vegetation and rainfall of bioclimatic ecoregions in central Africa. *Atmosphere* **2013**, *4*, 411–427. [CrossRef]
23. Boschetti, M.; Nutini, F.; Brivio, P.A.; Bartholomé, E.; Stroppiana, D.; Hościło, A. Identification of environmental anomaly hot spots in West Africa from time series of NDVI and rainfall. *ISPRS J. Photogramm. Remote Sens.* **2013**, *78*, 26–40. [CrossRef]
24. Bunting, E.L.; Southworth, J.; Herrero, H.; Ryan, S.J.; Waylen, P. Understanding Long-Term Savanna Vegetation Persistence across Three Drainage Basins in Southern Africa. *Remote Sens.* **2018**, *10*, 1013. [CrossRef]
25. Wingate, V.; Phinn, S.; Kuhn, N. Mapping precipitation-corrected NDVI trends across Namibia. *Sci. Total Environ.* **2019**, *684*, 96–112. [CrossRef]
26. Gilbert, E.; Reynolds, J.T. *Africa in World History*; Pearson Education: London, UK, 2011.
27. Els, M.J.T. Transfer pricing in Africa. *TaxTalk* **2012**, *2012*, 26–27.
28. Changara, M. Potential of Genetically Modified (gm) Crops to Increase Food Security on the African Continent. Available online: https://www.academia.edu/download/31416541/Potential_of_genetically_modified.pdf (accessed on 27 February 2021).
29. Davis-Reddy, C. *Assessing Vegetation Dynamics in Response to Climate Variability and Change across Sub-Saharan Africa*; Stellenbosch University: Stellenbosch, South Africa, 2018.
30. Steele, T. Late Pleistocene of Africa. In *Encyclopedia of Quaternary Science*; Elsevier BV: Amsterdam, The Netherlands, 2007; pp. 3139–3150.
31. Mousivand, A.; Arsanjani, J.J. Insights on the historical and emerging global land cover changes: The case of ESA-CCI-LC datasets. *Appl. Geogr.* **2019**, *106*, 82–92. [CrossRef]
32. Plummer, S.; LeComte, P.; Doherty, M. The ESA climate change initiative (CCI): A European contribution to the generation of the global climate observing system. *Remote Sens. Environ.* **2017**, *203*, 2–8. [CrossRef]
33. Wessels, K.J.; van den Bergh, F.; Scholes, R.J. Limits to detectability of land degradation by trend analysis of vegetation index data. *Remote Sens. Environ.* **2012**, *125*, 10–22. [CrossRef]
34. Zhu, Z.C.; Piao, S.L.; Myneni, R.B.; Huang, M.T.; Zeng, Z.Z.; Canadell, J.G.; Ciais, P.; Sitch, S.; Friedlingstein, P.; Arneth, A.; et al. Greening of the Earth and its drivers. *Nat. Clim. Chang.* **2016**, *6*, 791–795. [CrossRef]
35. Ibrahim, Y.Z.; Balzter, H.; Kaduk, J.; Tucker, C.J. Land degradation assessment using residual trend analysis of GIMMS NDVI3g, soil moisture and rainfall in sub-Saharan west Africa from 1982 to 2012. *Remote Sens.* **2015**, *7*, 5471–5494. [CrossRef]
36. Pinzon, J.; Tucker, C. Revisiting error, precision and uncertainty in NDVI AVHRR data: Development of a consistent NDVI3g time series. *Remote Sens.* **2013**. in preparation.
37. Tian, F.; Fensholt, R.; Verbesselt, J.; Grogan, K.; Horion, S.; Wang, Y.J. Evaluating temporal consistency of long-term global NDVI datasets for trend analysis. *Remote Sens. Environ.* **2015**, *163*, 326–340. [CrossRef]

38. Latifovic, R.; Pouliot, D.; Dillabaugh, C. Identification and correction of systematic error in NOAA AVHRR long-term satellite data record. *Remote Sens. Environ.* **2012**, *127*, 84–97. [CrossRef]
39. Dinku, T. Validation of the CHIRPS satellite rainfall estimate. in Seasonal Prediction of Hydro-Climatic Extremes in the Greater Horn of Africa. In Proceedings of the 7th International Precipitation Working Group (IPWG) Workshop, Tsukuba, Japan, 17–21 November 2014.
40. Funk, C.; Michaelsen, J.; Marshall, M.T. Mapping recent decadal climate variations in precipitation and temperature across eastern Africa. In *Remote Sensing of Drought: Innovative Monitoring Approaches*; CRC Press: Boca Raton, FL, USA, 2012; Volume 331.
41. Funk, C.; Verdin, A.; Michaelsen, J.; Peterson, P.; Pedreros, D.; Husak, G. A global satellite-assisted precipitation climatology. *Earth Syst. Sci. Data* **2015**, *7*, 275–287. [CrossRef]
42. Dinku, T.; Funk, C.; Peterson, P.; Maidment, R.; Tadesse, T.; Gadain, H.; Ceccato, P. Validation of the CHIRPS satellite rainfall estimates over eastern Africa. *Q. J. R. Meteorol. Soc.* **2018**, *144*, 292–312. [CrossRef]
43. Santoro, M.; Kirches, G.; Wevers, J.; Boettcher, M.; Brockmann, C.; Lamarche, C.; Defourny, P. *Land Cover CCI: Product User Guide Version 2.0*; Climate Change Initiative Belgium: Belgium, Leuven, 2017.
44. Jarvis, A. *Hole-Field Seamless SRTM Data*; International Centre for Tropical Agriculture (CIAT): Japan, Tokyo, 2008.
45. Pinzon, J.E.; Tucker, C.J. A non-stationary 1981–2012 AVHRR NDVI3g time series. *Remote Sens.* **2014**, *6*, 6929–6960. [CrossRef]
46. Herrmann, S.M.; Anyamba, A.; Tucker, C.J. Recent trends in vegetation dynamics in the African Sahel and their relationship to climate. *Glob. Environ. Chang.* **2005**, *15*, 394–404. [CrossRef]
47. Appelhans, T.; Detsch, F.; Nauss, T. Remote: Empirical orthogonal teleconnections in R. *J. Stat. Softw.* **2015**, *65*, 1–19. [CrossRef]
48. Zhou, L.; Tucker, C.; Kaufmann, R.K.; Slayback, D.; Shabanov, N.V.; Myneni, R. Variations in northern vegetation activity inferred from satellite data of vegetation index during 1981 to 1999. *J. Geophys. Res. Atmos.* **2001**, *106*, 20069–20083. [CrossRef]
49. Bogaert, J.; Zhou, L.; Tucker, C.J.; Myneni, R.B.; Ceulemans, R. Evidence for a persistent and extensive greening trend in Eurasia inferred from satellite vegetation index data. *J. Geophys. Res. Space Phys.* **2002**, *107*, ACL 4-1–ACL 4-14. [CrossRef]
50. Nzabarinda, V.; Bao, A.; Xu, W.; Uwamahoro, S.; Jiang, L.; Duan, Y.; Nahayo, L.; Yu, T.; Wang, T.; Long, G. Assessment and Evaluation of the Response of Vegetation Dynamics to Climate Variability in Africa. *Sustainability* **2021**, *13*, 1234. [CrossRef]
51. Olsson, L.; Eklundh, L.; Ardö, J. A recent greening of the Sahel—Trends, patterns and potential causes. *J. Arid Environ.* **2005**, *63*, 556–566. [CrossRef]
52. Dardel, C.; Kergoat, L.; Hiernaux, P.; Mougin, E.; Grippa, M.; Tucker, C. Re-greening Sahel: 30 years of remote sensing data and field observations (Mali, Niger). *Remote Sens. Environ.* **2014**, *140*, 350–364. [CrossRef]
53. Brandt, M.; Mbow, C.; Diouf, A.A.; Verger, A.; Samimi, C.; Fensholt, R. Ground-and satellite-based evidence of the biophysical mechanisms behind the greening Sahel. *Glob. Chang. Biol.* **2015**, *21*, 1610–1620. [CrossRef]
54. Masih, I.; Maskey, S.; Mussá, F.E.F.; Trambauer, P. A review of droughts on the African continent: A geospatial and long-term perspective. *Hydrol. Earth Syst. Sci.* **2014**, *18*, 3635–3649. [CrossRef]
55. Fensholt, R.; Rasmussen, K. Analysis of trends in the Sahelian 'rain-use efficiency' using GIMMS NDVI, RFE and GPCP rainfall data. *Remote Sens. Environ.* **2011**, *115*, 438–451. [CrossRef]
56. Berrahmouni, N.; Tapsoba, F.; Berte, C.J. The Great Green Wall for the Sahara and the Sahel Initiative: Building resilient landscapes in African drylands. In *Genetic Considerations in Ecosystem Restoration Using Native Tree Species*; Forest Assessment, Management and Conservation Division, Forestry Department, Food and Agriculture Organization of the United Nations: Rome, Italy, 2014; p. 15.
57. Diallo, M.D.; Goalbaye, T.; Mahamat-Saleh, M.; Sarr, P.S.; Masse, D.; Wood, S.A.; Diop, L.; Dick, R.P.; Diop, A.; Guisse, A. Effects of major woody species of the Senegalese Great Green Wall on N mineralization and microbial biomass in soils. *Bois For. Trop.* **2017**, *333*, 43–54.
58. Bader, J.; Latif, M. The 1983 drought in the West Sahel: A case study. *Clim. Dyn.* **2011**, *36*, 463–472. [CrossRef]
59. Calow, R.C.; Macdonald, A.M.; Nicol, A.L.; Robins, N.S. Ground water security and drought in Africa: Linking availability, access, and demand. *Ground Water* **2010**, *48*, 246–256. [CrossRef]
60. Nicholson, S.E. A detailed look at the recent drought situation in the Greater Horn of Africa. *J. Arid Environ.* **2014**, *103*, 71–79. [CrossRef]
61. UNOCHA. *Eastern Africa Drought*; Humanitarian Report; No 4, 2011; OCHA Eastern Africa: Nairobi, Kenya, 2011.
62. Ogutu, J.O.; Piepho, H.-P.; Dublin, H.T.; Bhola, N.; Reid, R.S. El Niño-southern oscillation, rainfall, temperature and normalized difference vegetation index fluctuations in the Mara-Serengeti ecosystem. *Afr. J. Ecol.* **2008**, *46*, 132–143. [CrossRef]
63. Nicholson, S.E. The nature of rainfall variability over Africa on time scales of decades to millenia. *Glob. Planet. Chang.* **2000**, *26*, 137–158. [CrossRef]
64. Ackerman, D.E.; Finlay, J.C. Road dust biases NDVI and alters edaphic properties in Alaskan arctic tundra. *Sci. Rep.* **2019**, *9*, 1–8. [CrossRef] [PubMed]
65. Pachauri, R.K.; Allen, M.R.; Barros, V.R.; Broome, J.; Cramer, W.; Christ, R.; Church, J.A.; Clarke, L.; Dahe, Q.; Dasgupta, P.; et al. *Climate Change 2014: Synthesis Report. Contribution of Working Groups I, II and III to the Fifth Assessment Report of the Intergovernmental Panel on Climate Change*; IPCC: Geneva, Switzerland, 2014.
66. Telesca, L.; Lasaponara, R. Pre-and post-fire behavioral trends revealed in satellite NDVI time series. *Geophys. Res. Lett.* **2006**, *33*. [CrossRef]

67. Telesca, L.; Lasaponara, R. Quantifying intra-annual persistent behaviour in SPOT-VEGETATION NDVI data for Mediterranean ecosystems of southern Italy. *Remote Sens.* **2006**, *101*, 95–103. [CrossRef]
68. Telesca, L.; Lasaponara, R. Discriminating dynamical patterns in burned and unburned vegetational covers by using SPOT-VGT NDVI data. *Geophys. Res. Lett.* **2005**, *32*. [CrossRef]
69. Fensholt, R.; Langanke, T.; Rasmussen, K.; Reenberg, A.; Prince, S.D.; Tucker, C.; Scholes, R.J.; Le, Q.B.; Bondeau, A.; Eastman, R.; et al. Greenness in semi-arid areas across the globe 1981–2007—An Earth Observing Satellite based analysis of trends and drivers. *Remote Sens. Environ.* **2012**, *121*, 144–158. [CrossRef]
70. Nemani, R.R.; Keeling, C.D.; Hashimoto, H.; Jolly, W.M.; Piper, S.C.; Tucker, C.J.; Myneni, R.B.; Running, S.W. Climate-driven increases in global terrestrial net primary production from 1982 to 1999. *Science* **2003**, *300*, 1560–1563. [CrossRef]
71. De Jong, R.; Schaepman, M.E.; Furrer, R.; De Bruin, S.; Verburg, P.H. Spatial relationship between climatologies and changes in global vegetation activity. *Glob. Chang. Biol.* **2013**, *19*, 1953–1964. [CrossRef]
72. Wu, D.H.; Zhao, X.; Liang, S.L.; Zhou, T.; Huang, K.C.; Tang, B.J.; Zhao, W.Q. Time-lag effects of global vegetation responses to climate change. *Glob. Chang. Biol.* **2015**, *21*, 3520–3531. [CrossRef] [PubMed]
73. Davenport, M.L.; Nicholson, S.E. On the relation between rainfall and the Normalized Difference Vegetation Index for diverse vegetation types in East Africa. *Int. J. Remote Sens.* **1993**, *14*, 2369–2389. [CrossRef]